THROMBOSIS AND HEMOSTASIS

Structure of the factor VIII C2 domain in a ternary complex with 2 inhibitor antibodies reveals classical and nonclassical epitopes

Justin D. Walter,[1] Rachel A. Werther,[1] Caileen M. Brison,[1] Rebecca K. Cragerud,[1] John F. Healey,[2] Shannon L. Meeks,[2] Pete Lollar,[2] and P. Clint Spiegel Jr[1]

[1]Western Washington University, Department of Chemistry, Bellingham, WA; and [2]Aflac Cancer and Blood Disorders Center, Department of Pediatrics, Emory University, Atlanta, GA

Key Points

- Antibodies against the factor VIII C2 domain inhibit procoagulant function.
- Crystal structure analysis of a C2 domain/antibody ternary complex describes epitopes for classical and nonclassical inhibitory antibodies.

The factor VIII C2 domain is a highly immunogenic domain, whereby inhibitory antibodies develop following factor VIII replacement therapy for congenital hemophilia A patients. Inhibitory antibodies also arise spontaneously in cases of acquired hemophilia A. The structural basis for molecular recognition by 2 classes of anti-C2 inhibitory antibodies that bind to factor VIII simultaneously was investigated by x-ray crystallography. The C2 domain/3E6 F_{AB}/G99 F_{AB} ternary complex illustrates that each antibody recognizes epitopes on opposing faces of the factor VIII C2 domain. The 3E6 epitope forms direct contacts to the C2 domain at 2 loops consisting of Glu2181-Ala2188 and Thr2202-Arg2215, whereas the G99 epitope centers on Lys2227 and also makes direct contacts with loops Gln2222-Trp2229, Leu2261-Ser2263, His2269-Val2282, and Arg2307-Gln2311. Each binding interface is highly electrostatic, with positive charge present on both C2 epitopes and complementary negative charge on each antibody. A new model of membrane association is also presented, where the 3E6 epitope faces the negatively charged membrane surface and Arg2320 is poised at the center of the binding interface. These results illustrate the potential complexities of the polyclonal anti-factor VIII immune response and further define the "classical" and "nonclassical" types of antibody inhibitors against the factor VIII C2 domain. (*Blood*. 2013;122(26):4270-4278)

Introduction

Congenital hemophilia A is an X-linked blood-clotting disorder resulting from dysfunction of blood coagulation factor VIII (fVIII), which affects 1 in 5000 males worldwide. The most effective treatment of congenital hemophilia A patients consists of regular prophylactic infusions of plasma-derived or recombinant fVIII.[1-3] However, a major impediment for fVIII replacement therapy is the development of inhibitory antibodies (inhibitors) against infused fVIII, a complication, which affects approximately 30% of severe hemophilia A patients.[4-6] By contrast, acquired hemophilia A is caused by an inhibitory autoimmune response to otherwise functional, endogenous fVIII.[7] FVIII inhibitors result in partially or fully inactivated fVIII, which results in loss of proper blood coagulation.

Blood coagulation fVIII is a 2332-residue glycoprotein with the domain arrangement A1-A2-B-A3-C1-C2.[8,9] In its inactive state, fVIII circulates as a heterodimer consisting of a heavy chain (A1-A2-B) and a light chain (A3-C1-C2) in a tightly bound complex with von Willebrand factor (VWF).[10-12] On proteolytic activation by thrombin or factor Xa, activated fVIII (fVIIIa) dissociates from VWF and binds specifically to phosphatidylserine (PS) on the extracellular surface of activated platelets.[13,14] After being bound to activated platelet surfaces, fVIIIa functions as a procoagulant cofactor for the serine protease factor IXa to form the intrinsic "tenase" complex, which dramatically accelerates the factor IXa-mediated activation of factor X by approximately 200 000-fold.[8,14,15]

The carboxy-terminal C2 domain of fVIII has been implicated in harboring the primary fVIII binding sites for both PS and VWF.[16,17] The binding of PS and VWF to C2 is mutually exclusive,[18-20] and numerous studies suggest this interaction involves 3 solvent-exposed hydrophobic loops protruding from the C2 domain β-sandwich core, including residues Met2199-Phe2200, Val2223, and Leu2251-Leu2252.[21-25] Several positively charged, basic residues encircle the base of these β-hairpin loops, and they may contribute to the interaction with the negatively charged PS headgroup.[22] In addition to interactions with phospholipid (PL) and VWF, there are previous reports that suggest the C2 domain contributes to the binding of thrombin and factor Xa to full-length fVIII, potentially acting as a docking module that may stabilize and promote the proteolytic activity of factor Xa/thrombin cleavages elsewhere in fVIII during activation.[26-28] Recent studies also suggest that the C1 domain contributes to binding both VWF and PS,[29,30] and deletion studies of the C2 domain indicate that it is not essential for PL membrane binding, factor IXa binding, or clotting activity.[31]

The C2 domain of fVIII is a major antigenic determinant for recognition by inhibitor antibodies.[32,33] Initial mechanistic investigations of anti-C2 inhibitor antibodies suggested that these antibodies

Submitted August 1, 2013; accepted September 30, 2013. Prepublished online as *Blood* First Edition paper, October 1, 2013; DOI 10.1182/blood-2013-08-519124.

The online version of this article contains a data supplement.

There is an Inside *Blood* commentary on this article in this issue.

The publication costs of this article were defrayed in part by page charge payment. Therefore, and solely to indicate this fact, this article is hereby marked "advertisement" in accordance with 18 USC section 1734.

Table 1. X-ray data collection and model refinement statistics

X-ray data statistics	
Wavelength (Å)	1.54
Resolution range (Å)	56.43-2.473 (2.561-2.473)
Space group	$P22_12_1$
Unit cell (Å)	a = 54.3, b = 71.2, c = 277.8
Total reflections	553 674 (78 388)
Unique reflections	39 550 (5 639)
Redundancy	14.0 (13.9)
Completeness (%)	99.9 (99.7)
I/σ(I)	11.7 (3.1)
R_{pim}	0.047 (0.230)
Model refinement statistics	
R_{factor}	0.1877 (0.2435)
R_{free}	0.2380 (0.3299)
Number of atoms	8 074
Protein	7 807
Water	267
Protein residues	1 016
RMS bonds (Å)	0.006
RMS angles (°)	0.88
Ramachandran favored (%)	96
Ramachandran outliers (%)	0.4
Average B-factor (Å²)	51.10
Protein	51.10
Solvent	50.70

prevent the binding of fVIII(a) to PL and VWF.[34-37] A 2.0 Å crystal structure of the human C2 domain bound to 1 such "classical" inhibitor antibody, BO2C11, showed that key C2 residues thought to be involved with PL and VWF binding are occluded by the C2-BO2C11 interface.[25] However, recent evidence suggests that a separate class of "nonclassical" anti-C2 antibodies allows binding of the C2 domain to PL/VWF, but inhibits the activation of fVIII by thrombin or factor Xa.[38-40] Interestingly, a large panel study showed that nonclassical inhibitors represented the highest frequency of occurrence among anti-C2 antibodies in inhibitor plasma from hemophilia A mice inoculated with human fVIII, and they are pathogenic in a murine tail snip bleeding model.[38,40] Moreover, it was also found that nonclassical anti-C2 antibodies are present in the majority of human polyclonal anti-C2 inhibitor plasmas.[39] Therefore, nonclassical inhibitors represent a significant component of the human pathogenic anti-fVIII immune response.

In this study, we report a 2.47 Å x-ray crystal structure of the human fVIII C2 domain in a ternary complex with 2 antigen binding fragments (F_{AB}s) of monoclonal antibodies (mAbs) to a classical epitope (3E6) and a nonclassical epitope (G99). This structure provides the first high-resolution glimpse of a nonclassical epitope on the surface of C2, and also expands the understanding of the binding modes of classical inhibitors. Moreover, our crystal structure confirms the suggested epitope regions previously characterized by small-angle x-ray scattering (SAXS) analysis.[41] This study, along with previous work,[38] establishes 3E6 and G99 as epitope probes, which have the potential to define further the role of specific regions of the fVIII C2 domain in procoagulant function and antibody recognition.

Materials and methods

Protein purification and complex formation

The fVIII C2 domain was expressed and purified as previously described.[41-43] Monoclonal anti-human fVIII C2-specific antibodies (3E6 and G99) were produced from hybridomas following immunization of hemophilia A mice with intravenous, adjuvant-free injections of human fVIII, as described previously.[38,41] Large-scale antibody production was performed at the Antibody Production Facility at the Fred Hutchinson Cancer Research Center (FHCRC) (E. Wayner, Seattle, WA). Immunoglobulin (IgG) and F_{AB} purifications were completed with the NAb Protein A Plus spin column and immobilized papain kits (Thermo Scientific, Rockford, IL) according to the manufacturer's protocols. F_{AB} fragments were purified further with a Superdex 75 column in F_{AB} storage buffer [25 mM Tris-HCl pH 7.2, 100 mM NaCl]. The fVIII C2 domain/3E6/G99 F_{AB} ternary complex was formed by equimolar addition of each protein component at 37°C for 30 minutes, followed by purification of the ternary complex by size exclusion with a Superdex 75 column.

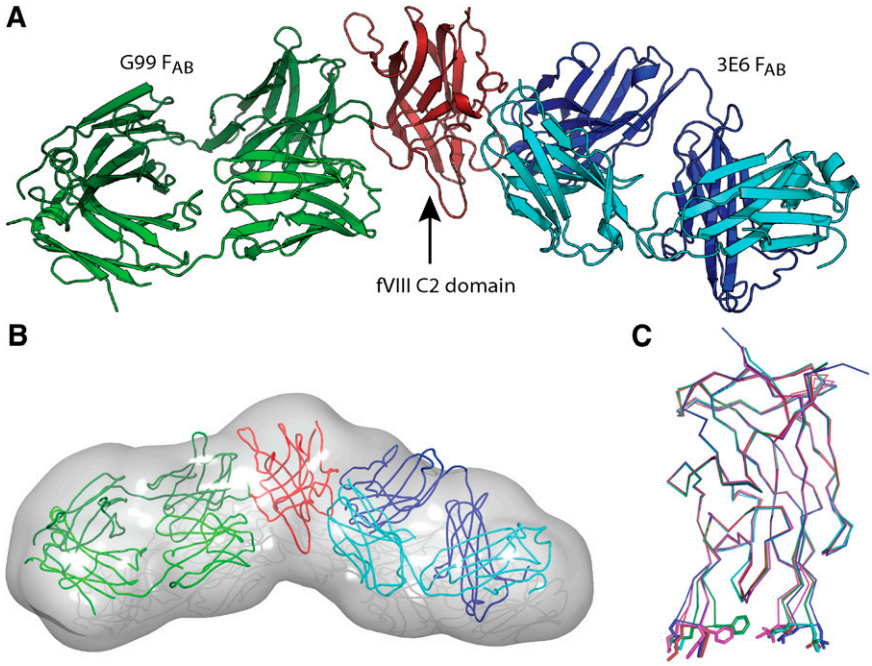

Figure 1. X-ray crystal structure of the FVIII C2 domain/3E6 FAB/G99 FAB ternary complex. (A) Ribbon diagram presentation of the ternary complex determined to 2.47 Å resolution (pdb# 4KI5); red: fVIII C2 domain, blue: 3E6 F_{AB} heavy chain, cyan: 3E6 F_{AB} light chain, dark green: G99 F_{AB} heavy chain, light green: G99 F_{AB} light chain. (B) Rigid body modeling of the ternary crystal structure into the previously calculated SAXS-derived molecular envelope (colors same as in A). (C) Superposition of different x-ray crystal structures of the fVIII C2 domain. Red: ternary complex C2 domain (pdb# 4KI5), blue: pdb# 1D7P, green: pdb# 3HNB, cyan: pdb# 3HNY, magenta: pdb# 3HOB. The side chains of solvent exposed hydrophobic loops are displayed (Met2199, Phe2200, Leu2251, Leu2252).

Crystallization and x-ray structure determination

Crystals of the C2/3E6/G99 ternary complex were produced by hanging drop vapor diffusion at 2 mg/mL by mixing 2 μL protein complex [25 mM Tris-HCl, pH 7.5, and 50 mM NaCl] with 2 μL of reservoir solution [28% PEG 1000, 0.15 M sodium acetate pH 3.6, and 0.15 M ammonium nitrate] at room temperature. Crystals were flash frozen in liquid nitrogen in the same solution, following the addition of 30% (vol/vol) glycerol as a cryoprotectant. X-ray diffraction data were collected to 2.47 Å resolution on a Rigaku Micromax-007HF rotating anode with Confocal Varimax Optics Systems and an RAXIS-IV++ imaging plate detector at the FHCRC (Seattle, WA). Data collection, indexing, and scaling of diffraction data were performed with CrystalClear, MOSFLM, and SCALA software, respectively.[44] Initial phases were determined with PHASER via molecular replacement, using previously determined crystal structures for the isolated C2 domain (PDB: 1D7P) and separate searches for the variable and constant domains of an F_{AB} fragment, in which the CDR loops were deleted (PDB: 1IQD) as search models. Iterative cycles of model building and refinement were performed with COOT and PHENIX, respectively.[45,46] F_{AB} variable regions were built according to the determined sequences (Genscript, Piscataway, NJ), and the constant regions were built corresponding to the conserved consensus sequences of murine antibody isotype IgG2aκ. Validation of the final refined model was performed with Molprobity.[47] Electrostatic calculations were performed with APBS.[48] Molecular structure figures were generated with Chimera and PyMol.[49]

Results

X-ray crystal structure of the ternary complex

A ternary complex consisting of the human fVIII C2 domain bound to the F_{AB} fragments purified from anti-human fVIII mAbs, 3E6 and G99, was purified, characterized, and crystallized as described in "Material and methods." The x-ray crystal structure of the fVIII C2 domain/3E6/G99 ternary complex was determined to a resolution of 2.47 Å (Table 1). Calculated electron density maps allowed for modeling of the majority of residues, with the exception of the C2 domain hexahistidine affinity tag, the amino- and carboxy-termini of the C2 domain (residues 2171-2173 and 2328-2332), residues 198-199 within the 3E6 F_{AB}, and residues 199-202 within the G99 F_{AB}. Electron density corresponding to the C2/F_{AB} interfaces was of high quality, allowing for the unambiguous modeling of all C2/F_{AB} contacts. The complete tertiary structure of the complex shows that each F_{AB} recognizes opposing faces of the fVIII C2 domain, as previously suggested (Figure 1A).[41] Interestingly, the overall morphology and geometry of the ternary complex agrees well with a recently described low-resolution SAXS model, with a measured angle between antibodies of ~135° (Figure 1B).[41] Buried surface areas for each anti-fVIII epitope were calculated to be approximately 690 $Å^2$ and 810 $Å^2$ between the fVIII C2 domain and the 3E6 and G99 interfaces, respectively. Cumulatively, the 2 F_{AB}s bury approximately 20% of the total fVIII C2 domain surface area. Superposition of the C2 domain from the 3E6/G99 ternary complex with previously determined x-ray crystal structures of the fVIII C2 domain (PDB ID#: 1D7P, 3HNB, 3HNY, 3HOB) indicate that the tertiary structure of the fVIII C2 domain is highly conserved (Figure 1C), with the largest deviation occurring at the hydrophobic hairpin loops (residues Met2199, Phe2200, Leu2251, and Leu2252), which are not direct contacts within either epitope, and are previously determined to be highly dynamic.[23,25,50]

FVIII C2 domain interactions with the classical antibody, 3E6

Inspection of the binding interfaces between the fVIII C2 domain and each antibody, 3E6 and G99, shows key regions of the C2 domain involved in antibody recognition. A complete description of direct atomic contacts between the C2 domain and each antibody is listed in Table 2, and a list of C2 domain residues for which solvent accessibility is decreased on 3E6 or G99 binding is also presented (supplemental Table 1, available on the *Blood* Web site).[51] The 3E6 F_{AB} occludes 2 distinct regions of the C2 domain, encompassing loops consisting of residues Glu2181-Ala2188 and Thr2202-Arg2215 (Figure 2). Within this discontinuous epitope, 7 C2 residues are positioned to make direct contact with 3E6, including Lys2183, Asp2187, Arg2209, His2211, Gln2213, Gly2214, and Arg2215 (Table 2). Two of these residues, Lys2183 and Gln2213, appear to make especially robust contributions to the C2-3E6 interface, where greater than 80% of their exposed surface area is buried on binding the 3E6 F_{AB} (supplemental Table 1). Lys2183 is within hydrogen bonding distance of 2 residues within the 3E6 F_{AB} light chain, and is juxtaposed with Trp90 of the 3E6 light chain in such a manner that suggests a cation-π interaction (Figure 2A). The positioning of Gln2213 places side chain atoms within close contact of 4 different residues within the 3E6 heavy chain, with direct hydrogen bonding to Thr53 and Ser33 (Figure 2B).

Table 2. Direct C2 domain/antibody contacts in the ternary complex

C2 residue	F_{AB}, Chain	F_{AB} residue	Distance (Å)
K2183 NZ	3E6, Light	W90 O	3.04
O		Y93 N	2.94
D2187 N	3E6, Light	S91 O	2.81
OD1		S30 OG	2.55
		S91 OG	3.63
S2194 OG	G99, Light	Y32 OH	3.53
R2209 NH2	3E6, Light	S91 O	3.88
H2211 O	3E6, Heavy	N52 ND2	2.93
ND1		T55 OG1	3.73
Q2213 NE2	3E6, Heavy	T30 O	3.13
		Y32 O	3.57
		N52 OD1	3.82
		T53 OG1	2.78
		S33 OG	2.70
		N52 ND2	3.64
OE1		T53 N	3.06
G2214 N	3E6, Heavy	D31 O	2.91
R2215 NE	3E6, Heavy	D100 OD2	3.86
NH1		T32 OH	3.69
		D100 OD1	2.87
		OD2	3.24
NH2		D100 OD1	3.32
		OD2	2.94
		D101 OD2	3.82
Q2222 NE2	G99, Light	S30 OG	3.51
N2225 ND2	G99, Light	Y91 O	3.74
		A92 O	2.81
K2227 NZ	G99, Light	Y94 OH	3.11
		Y96 OH	2.88
	G99, Heavy	E50 OE1	3.49
	G99, Heavy	T99 OG1	2.92
O		F103 N	2.84
E2228 OE2	G99, Light	Y32 OH	2.83
W2229 NE1	G99, Heavy	F103 O	2.68
S2263 OG	G99, Heavy	Y101 OH	3.73
V2280 N	G99, Heavy	G54 O	2.81

FVIII C2 domain interactions with the nonclassical antibody, G99

The G99 F_{AB} recognizes a structurally more complex epitope than 3E6, burying fVIII C2 domain residues residing in 5 distinct

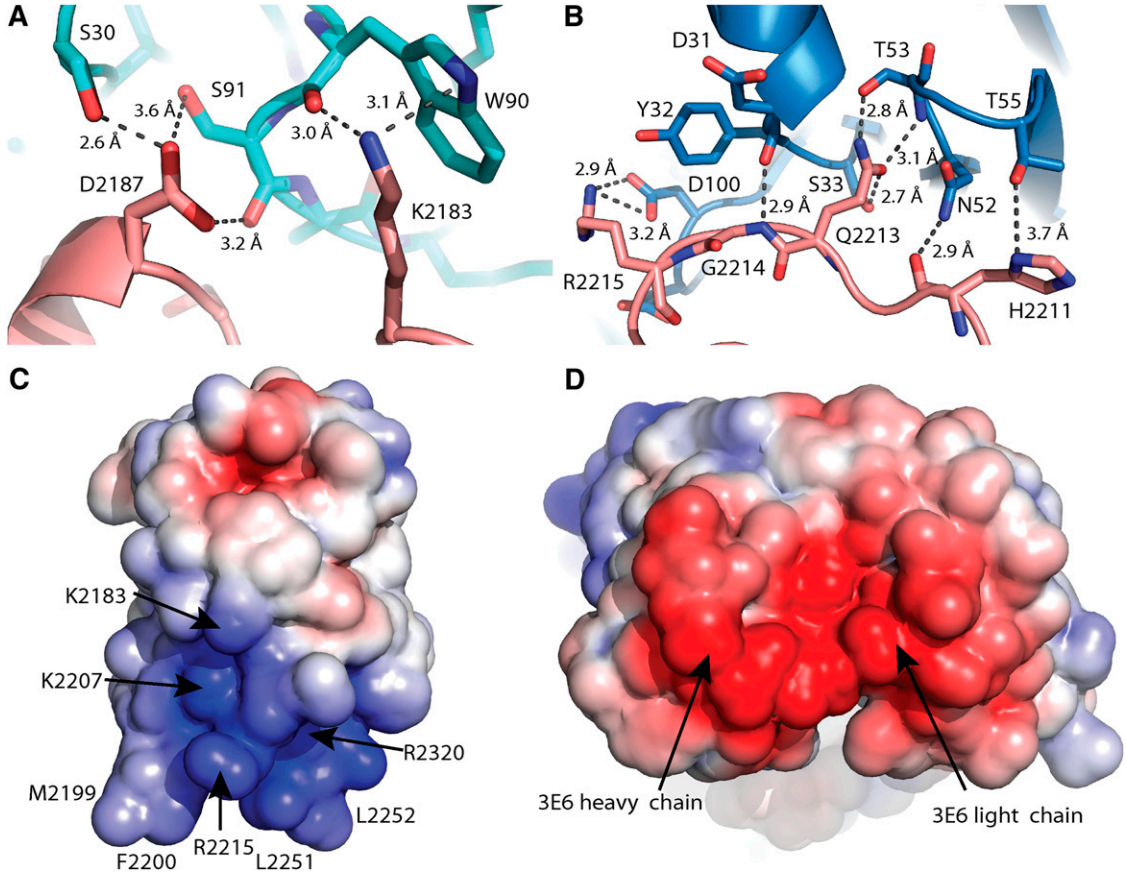

Figure 2. The fVIII C2 domain/3E6 F_{AB} interface. (A) Direct molecular contacts between the 3E6 light chain and C2 domain residues Lys2183/Asp2187; pink: fVIII C2 domain, cyan: 3E6 light chain. (B) Direct molecular contacts between the 3E6 heavy chain and the C2 domain 2211-2215 loop; pink: fVIII C2 domain, blue: 3E6 heavy chain. (C,D) Electrostatic surface potentials for the 3E6 epitope on the fVIII C2 domain (C) and the variable region of the 3E6 F_{AB} (D); blue: positive charge, red: negative charge. The surface potentials were calculated with APBS at surface potential values of ±5 kT/e, and the surfaces were displayed in PyMol.

regions: Ser2193-Ser2194, Gln2222-Trp2229, Leu2261-Ser2263, His2269-Val2282, and Arg2307-Gln2311 (Figure 3). The G99 F_{AB} forms direct contacts with 8 C2 residues: Ser2194, Gln2222, Asn2225, Lys2227, Glu2228, Trp2229, Ser2263, and Val2280. In a striking fashion, the G99 epitope is centered on Lys2227, where several side chains of both the heavy (Glu50 and Thr99) and light (Tyr94 and Tyr96) chains of the G99 antibody form direct hydrogen bonds to the primary amine group of Lys2227 (Figure 3A). Additionally, Lys2227 is positioned proximally to Trp33 of the G99 heavy chain for a cation-π interaction. Adjacent to Lys2227, residues Gln2222, Asn2225, and Glu2228 make direct electrostatic interactions with Ser30, Ala92, and Tyr32 of the G99 light chain, respectively (Figure 3B). In contrast to the 3E6 epitope, the C2 domain/G99 binding interface buries more hydrophobic surface area. Specifically, C2 residues Val2223 (81%), Leu2273 (93%), Phe2275 (29%), Val2280 (92%), and Val2282 (37%) bury more than 25% of their respective surface area on complex formation with the G99 antibody (Figure 3B,C).

Electrostatic contributions to antibody recognition of the FVIII C2 domain

Inspection of the binding interfaces between the fVIII C2 domain and the 3E6 and G99 antibodies shows that the majority of interactions are electrostatic in nature, with multiple hydrogen bonds and salt bridges forming each C2/F_{AB} interface. Calculation and analysis of solvent accessible electrostatic surface potentials for each C2/F_{AB} complex dramatically illustrates the respective contributions of electrostatics to the binding interface. The basic side chain of Arg2215 protrudes into the bottom of the acidic binding cleft between the heavy and light chain CDR loops of the 3E6 F_{AB} (Figure 2C,D). Adjacent to Arg2215 reside both Lys2207 and Arg2320, and Lys2183 anchors the top of the binding interface, all of which contribute to the largely basic character of the 3E6 epitope. Although the total electrostatic potential of the C2/G99 interface is weaker than the 3E6 interface, it dramatically shows a deep acidic pocket, which precisely accommodates the basic side chain of Lys2227 (Figure 3C,D). Within this binding cleft, 3 G99 residues are poised to form hydrogen bonds with the primary amine group of Lys2227, as well as a glutamate moiety, Glu50, which appears to form a salt bridge interaction (Figure 3A, Table 2).

Discussion

The C2 domain of fVIII is a major recognition site for inhibitory antibodies.[32,33] The present study is an examination of an x-ray crystal structure of the human fVIII C2 domain in a ternary complex with F_{AB} fragments from 2 anti-human fVIII inhibitor antibodies, 3E6 and G99, that were isolated from hemophilia A mice.[38] The 3E6 mAb is a classical inhibitor, defined as an antibody that inhibits the binding of fVIII and the C2 domain to PL surfaces and/or VWF. By contrast, the G99 mAb is a nonclassical inhibitor, which inhibits the

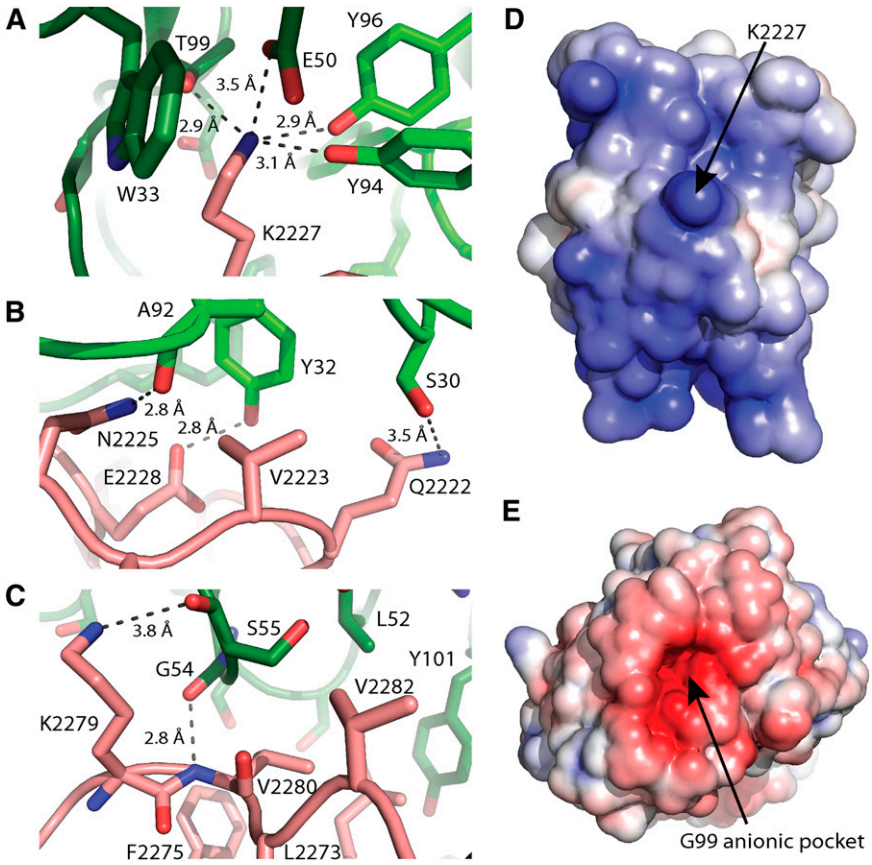

Figure 3. The FVIII C2 domain/G99 F_{AB} interface. (A) Direct molecular contacts between the G99 CDR region and C2 domain residue Lys2227; pink: fVIII C2 domain, dark green: G99 heavy chain, light green: G99 light chain. (B) Direct molecular contacts between the G99 light chain and the C2 domain 2222-2228 loop; pink: fVIII C2 domain, light green: G99 light chain. (C) Direct molecular contacts between the G99 heavy chain and the C2 domain residues 2273-2282; pink: fVIII C2 domain, dark green: G99 heavy chain. (D,E) Electrostatic surface potentials for the G99 epitope on the fVIII C2 domain (D) and the variable region of the G99 F_{AB} (D); blue: positive charge, red: negative charge. The surface potentials were calculated with APBS at surface potential values of ±5 kT/e, and the surfaces were displayed in PyMol.

activation of fVIII by thrombin or factor Xa, delaying procoagulant function and resulting in the inability of fVIII to dissociate from VWF. Previous data have suggested that various classical/nonclassical anti-C2 antibodies cooperatively bind, and inhibit, the full-length fVIII (P. Lollar and S. L. Meeks, unpublished observations). High-resolution structure determinations such as the work presented herein allow for detailed description of C2 domain epitopes and provide further structural information regarding the function of the fVIII C2 domain in the coagulation cascade.

The x-ray crystal structure of the C2 domain/3E6/G99 ternary complex directly illustrates that each antibody binds to opposing sides of the fVIII C2 domain, which is consistent with previous antibody competition experiments as well as SAXS studies (Figure 1A,B).[38,41] The 3E6 epitope partially consists of Lys2183, Asp2187, and Arg2215, each of which is expected to be involved in VWF binding (Figure 2).[52] Moreover, Lys2183 forms a direct contact with multiple 3E6 residues and is largely buried at the binding interface (Figure 2A), which is consistent with a Lys2183Ala mutant that decreases 3E6 binding by an order of magnitude.[41] By contrast, multiple residues at the C2 domain/G99 interface are suggested to be involved in binding both factors IXa and Xa. Specifically, Glu2228 and Trp2229 form direct contacts to G99 (Figure 3B), which are predicted to be involved in factor IXa binding by the fVIII C2 domain.[53,54] Additionally, a hydrophobic region containing Leu2261, Ser2263, and Phe2265, which is shown to be buried in the C2 domain/G99 interface (Figure 3C), has previously been reported to bind factor Xa.[27] As stated earlier, however, the strongest region of fVIII C2 domain recognition by G99 is Lys2227, which is completely buried in the C2 domain/G99 interface and forms multiple electrostatic interactions (Figure 3A). Supporting mutagenesis studies indicate that the Lys2227Ala mutation completely abrogates binding of G99 to fVIII.[38] Further mutagenesis and structure/function studies are needed to understand the physiological relevance of the binding of factors IXa and Xa to the fVIII C2 domain.

Perhaps the most unexpected result is the observation that neither of the antibodies binds to the region containing the solvent-exposed hydrophobic loops, which contain Met2199/Phe2200 and Leu2251/Leu2252.[23] Previous structural findings strongly suggest that these 2 loops are an important determinant for PL binding, where the first structurally characterized anti-fVIII antibody BO2C11 binds and potently inhibits the binding of the fVIII C2 domain to both PL and VWF.[25,34] Superposition of the C2 domains from the fVIII C2/BO2C11 F_{AB} structure with the ternary structure reported herein illustrates each of the epitopes and the associated overlap between them. Interestingly, the epitope overlap is greater between BO2C11 and G99 than for the BO2C11 and 3E6 (Figure 4A), which is not consistent with the previous observation that BO2C11 competes with 3E6 but not G99 for binding to fVIII.[38] Nevertheless, both BO2C11 and 3E6 mAbs, but not G99, inhibit the ability of fVIII to bind both PL and VWF.[34,38] Given the structural epitopes identified in the present study, we are able to refine a working structural model for how the fVIII C2 domain binds to PL surfaces. In contrast to previous models that include the G99 structural epitope (Figure 3) in membrane binding,[23,50,55] our working model for PL membrane binding involves direct interaction of both the BO2C11 and 3E6 epitopes, which leaves both hydrophobic loops still making direct contacts with the PL membrane interior, but basic residues of the 3E6 side of the C2 domain are now poised to interact directly with the negative charge of the PS headgroup (Figure 4B). We further hypothesize that the polar PS headgroup interacts directly with the binding cleft that contains Arg2320 at its base, which displays the highest positive electrostatic potential on the surface of the fVIII C2

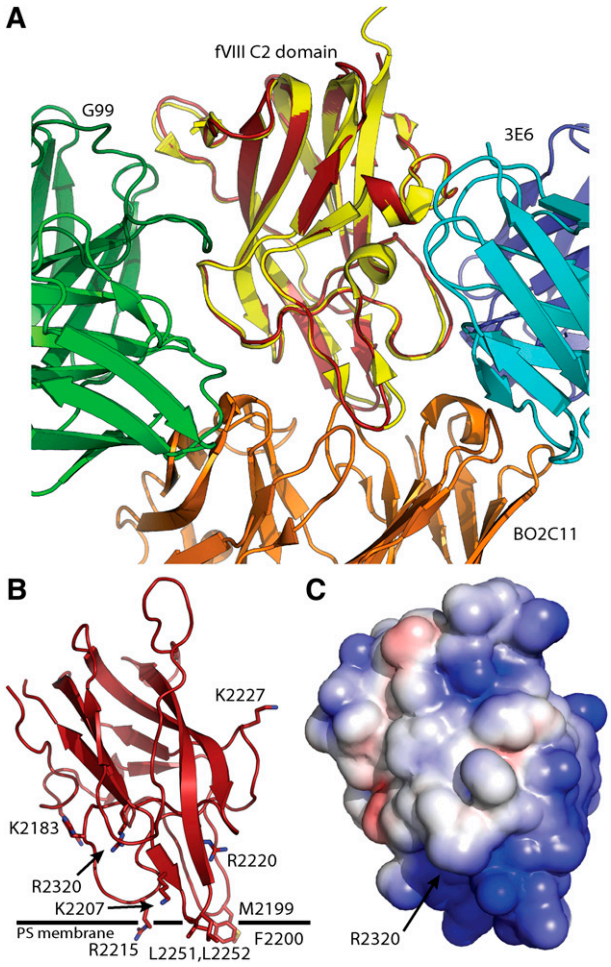

Figure 4. Anti-fVIII C2 domain epitope mapping and modeling of PL membrane binding. (A) Superposition of the C2 domain/3E6/G99 ternary complex with the C2 domain/BO2C11 binary complex; red: ternary complex C2 domain, yellow: BO2C11-bound C2 domain, green: G99 F_{AB}, blue/cyan: 3E6 F_{AB}, orange: BO2C11 F_{AB}. The BO2C11 and 3E6 antibodies inhibit binding of fVIII to PL membranes. (B,C) Model for PL membrane association by the fVIII C2 domain based on epitope mapping; (B) ribbon diagram with basic and surface-exposed hydrophobic residues and proposed PL membrane position highlighted; (C) electrostatic surface potential for the fVIII C2 domain in the same orientation as in B, blue: positive charge, red: negative charge. The surface potentials were calculated and displayed as in Figures 2 and 3.

domain (Figure 4C). The observation that Arg2320 is highly conserved, not only in the C2 domain but also in the C1 domain, supports this hypothesis. Previous mutagenesis data partially support this hypothesis, where multiple residues involved in both 3E6 and G99 binding (Arg2209, Gln2213, Arg2215, Val2223, and Lys2227) are important for PL binding.[21] Although these results carry weight because of the data being collected with full-length fVIII constructs, the study is limited in its scope as a result of mutagenesis limitations (eg, the Arg2320 full-length fVIII mutant was not active). An alternative hypothesis is that classical antibodies, such as 3E6, do not directly bind to the region interacting with PL surfaces, but rather result in charge neutralization on antibody binding, which decreases membrane binding because of long-range electrostatic effects. Visualization of the electrostatic surface potential for both the C2/3E6 and the C2/G99 binary structures supports this hypothesis (supplemental Figure 1), which is consistent with previous hypotheses regarding antibody inhibition of VWF binding.[52,56] A third hypothesis is that the binding of 3E6 affects the dynamics of the fVIII C2 domain, which could modify flexible loops that may be important to allow membrane engagement. Analysis of the crystallographic thermal B factors does not support this hypothesis, however, as the average B factors for the 2 hydrophobic loops (2199/2200 and 2251/2252) display higher than average values, which are often concomitant with dynamic flexibility.[57]

One recurring observation for each fVIII C2 domain inhibitory antibody studied thus far is the importance of electrostatics. Each epitope consists of highly basic surface electrostatic potential that is complemented dramatically by each inhibitory antibody (Figures 2C,D and 3D,E). On visualization of the binding interface, each structure is highly charged with direct contact salt bridges being important structural determinants for each antibody. Aside from the highly charged interactions that are observed for each of the anti-C2 antibodies, there are varying amounts of buried hydrophobic surface area. The 3E6 antibody interface contains a minimal amount of hydrophobic surface area, whereas the G99 antibody recognizes 1 hydrophobic patch Figure 3C), and the BO2C11 completely sequesters both hydrophobic solvent exposed loops in the binding interface.[25] Both the 3E6 and G99 antibodies bury similar amounts of total surface area (690 $Å^2$ and 810 $Å^2$, respectively), and possess similar values for apparent equilibrium dissociation constants (3.2 nM and 8.1 nM, respectively).[41]

The in vitro potency of fVIII inhibitors is measured by the Bethesda assay, in which 1 Bethesda unit (BU) per mL is defined as the dilution of test substance that produces 50% inhibition of activity in a fVIII assay.[58] Inhibitors are further characterized as Type I or Type II depending on whether they completely or incompletely inhibit fVIII at saturating concentrations of antibody.[59] Interestingly, the 3E6 antibody is a significantly weaker inhibitor of fVIII cofactor activity compared to the G99 antibody, where the inhibitor titers for each mAb are 41 BU/mg and 15 000 BU/mg, respectively.[38] Previous studies of the different classes of anti-fVIII C2 antibodies illustrate that inhibitor titer discrepancy is a common observation. Notably, classical C2 antibodies typically are low-titer type I inhibitors, and nonclassical antibodies typically are high-titer type II inhibitors, yet classical antibodies are more pathogenic in bleeding models.[38-40,60] One dramatic exception to this observation is the BO2C11 antibody inhibitor. The BO2C11 is a classical anti-C2 inhibitor that buries significantly more surface area (~1100 $Å^2$), binds fVIII with an equilibrium dissociation constant of 14 pM, and possesses an inhibitor titer of 20 000 BU/mg.[34,38] Furthermore, the BO2C11 has IC_{50} values for both VWF and PL binding that are approximately 2 orders of magnitude less than that for the 3E6 antibody.[34,38] It is evident that the BO2C11 and 3E6 antibodies, although both considered "classical," behave differently.[38] One possible interpretation is that 3E6 functions similarly to the ESH4 antibody, which has an overlapping epitope with 3E6.[38] ESH4 has been reported to decrease the apparent membrane affinity of fVIII by approximately 10-fold and decrease the maximal catalytic function of the intrinsic tenase complex, as opposed to complete inhibition of membrane binding.[30] In contrast to ESH4 (which is a type II inhibitor), 3E6 appears to completely inhibit PS binding and factor Xa generation, is a type I inhibitor, and the F_{AB} displays similar potency to IgG in Bethesda assays.[38,41]

The defined epitopes for each of the structurally characterized antibodies have been designated anti-C2 inhibitors, but it is not clear whether or not the 3E6, G99, or BO2C11 antibodies have steric overlap with other regions of fVIII. As visualized in Figure 5, superposition of the C2 domains from the ternary complex structure presented in this study with the BO2C11/C2 domain complex structure and the B domain-deleted fVIII structure shows there is no steric overlap between any of the antibodies and the remaining

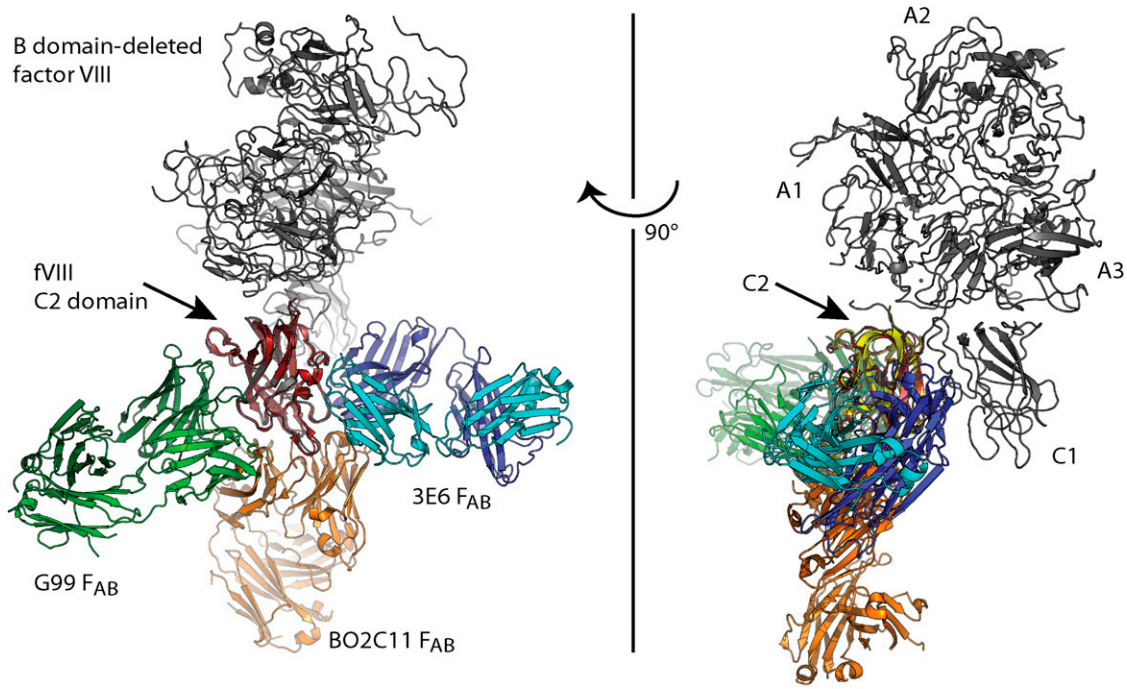

Figure 5. Modeling anti-C2 domain antibodies onto the x-ray crystal structure of full-length FVIII. Superposition of each C2 domain from the C2/3E6/G99 ternary structure, the C2/BO2C11 binary structure, and the full-length B domain-deleted fVIII crystal structure (pdb# 2R7E) indicated no steric overlap between any F_{AB} fragments and the remaining structure of fVIII. Full-length fVIII is shown in gray, red: C2 domain, orange: BO2C11 F_{AB}, green: G_{99} F_{AB}, blue/cyan: 3E6 F_{AB}.

structure of fVIII (Figure 5).[24,34] These structural findings support the validity of employing single domains (such as the fVIII C2 domain in this study) to understand the immune response associated with hemophilia A treatment. Moreover, the lack of steric overlap contributes further evidence that the x-ray crystal structure of the B domain-deleted fVIII is a physiologically relevant structure that is present in circulation. The positioning of the C1 domain relative to the C2 domain supports previous data indicating that the C1 domain contributes to membrane association and the C2 domain is not essential for function.[29-31] Lastly, the x-ray crystal structure of the C2 domain/3E6/G99 complex is remarkably similar to the previously modeled ternary complex from low-resolution SAXS data (Figure 1B).[41] These structural findings suggest that using rapid, low-resolution techniques such as SAXS may be effective tools for characterizing other antibody epitopes for fVIII inhibitor antibodies as well as other antigen/antibody interactions. Additionally, the solution phase SAXS structure supports and validates the solid phase x-ray crystal structure.

The development of an immune response against blood coagulation fVIII remains the most significant complication from treatment of inherited hemophilia A and is the underlying cause of acquired hemophilia A. High-resolution structural findings such as the x-ray crystal structure presented in this study provide detailed information regarding fVIII epitopes, which can now be cross referenced against inhibitory frequency, potency, and pathogenicity. Moreover, the observation that 2 different antibodies recognize the fVIII C2 domain simultaneously, and in some cases cooperatively, necessitates further study of the polyclonal antibody response to fVIII to understand the complex nature of the immune response and its associated pathogenicity. Future investigations concerning the relative importance of each surface exposed basic and hydrophobic region within the fVIII C2 domain may lead to next-generation recombinant fVIII products that display decreased immunogenicity. Furthermore, studies of anti-fVIII antibody epitopes, and their associated activities, also contribute to understanding the mechanism of fVIII procoagulant function. Subsequent investigations concerning antibody inhibitors that target other regions of fVIII will yield important structural information regarding the formation and activity of the intrinsic "tenase" complex in blood coagulation as well as provide further understanding of the immune response to blood coagulation fVIII.

Acknowledgments

We are grateful to Barry Stoddard at the FHCRC for providing x-ray diffraction facilities and to Dr Elizabeth Wayner and the antibody productions facility at the FHCRC for producing antibodies.

This work was supported by the National Institutes of Health grant R15 HL103518 (P.C.S.), the National Science Foundation (CHE-1062722), by National Institutes of Health grants U54 HL112309 and K08 HL102262 and Hemophilia of Georgia, Inc. (S.L.M.), and National Institutes of Health grants U54 HL112309, R01 HL082609, and R01 HL040921 and Hemophilia of Georgia, Inc. (P.L.).

Authorship

Contribution: J.D.W. designed and performed research, analyzed data, and cowrote the manuscript; R.A.W., C.M.B., and R.K.C. purified proteins and characterized antigen/antibody complexes; J.F.H. generated and characterized antibodies; S.L.M., P.L., and P.C.S. designed research, analyzed data, and co-wrote the manuscript.

Conflict-of-interest disclosure: The authors declare no competing financial interests.

Correspondence: P. Clint Spiegel Jr, Department of Chemistry, Western Washington University, 516 High St, Bellingham, WA 98225; e-mail: spiegep@chem.wwu.edu.

References

1. Hoots WK. The future of plasma-derived clotting factor concentrates. *Haemophilia.* 2001; 7(Suppl 1):4-9.
2. Mauser-Bunschoten EP, van der Bom JG, Bongers M, Twijnstra M, Roosendaal G, Fischer K, van den Berg HM. Purity of factor VIII product and incidence of inhibitors in previously untreated patients with haemophilia A. *Haemophilia.* 2001; 7(4):364-368.
3. Scharrer I, Bray GL, Neutzling O. Incidence of inhibitors in haemophilia A patients—a review of recent studies of recombinant and plasma-derived factor VIII concentrates. *Haemophilia.* 1999;5(3): 145-154.
4. Bray GL, Gomperts ED, Courter S, et al; The Recombinate Study Group. A multicenter study of recombinant factor VIII (recombinate): safety, efficacy, and inhibitor risk in previously untreated patients with hemophilia A. *Blood.* 1994;83(9): 2428-2435.
5. Kreuz W, Ettingshausen CE, Zyschka A, Oldenburg J, Saguer IM, Ehrenforth S, Klingebiel T. Inhibitor development in previously untreated patients with hemophilia A: a prospective long-term follow-up comparing plasma-derived and recombinant products. *Semin Thromb Hemost.* 2002;28(3):285-290.
6. Lusher JM, Lee CA, Kessler CM, Bedrosian CL; ReFacto Phase 3 Study Group. The safety and efficacy of B-domain deleted recombinant factor VIII concentrate in patients with severe haemophilia A. *Haemophilia.* 2003;9(1):38-49.
7. Franchini M, Lippi G. Acquired factor VIII inhibitors. *Blood.* 2008;112(2):250-255.
8. Gitschier J, Wood WI, Goralka TM, et al. Characterization of the human factor VIII gene. *Nature.* 1984;312(5992):326-330.
9. Toole JJ, Knopf JL, Wozney JM, et al. Molecular cloning of a cDNA encoding human antihaemophilic factor. *Nature.* 1984;312(5992): 342-347.
10. Foster PA, Fulcher CA, Marti T, Titani K, Zimmerman TS. A major factor VIII binding domain resides within the amino-terminal 272 amino acid residues of von Willebrand factor. *J Biol Chem.* 1987;262(18):8443-8446.
11. Hill-Eubanks DC, Parker CG, Lollar P. Differential proteolytic activation of factor VIII-von Willebrand factor complex by thrombin. *Proc Natl Acad Sci USA.* 1989;86(17):6508-6512.
12. Lenting PJ, van Mourik JA, Mertens K. The life cycle of coagulation factor VIII in view of its structure and function. *Blood.* 1998;92(11): 3983-3996.
13. Lollar P, Parker CG. Subunit structure of thrombin-activated porcine factor VIII. *Biochemistry.* 1989;28(2):666-674.
14. van Dieijen G, Tans G, Rosing J, Hemker HC. The role of phospholipid and factor VIIIa in the activation of bovine factor X. *J Biol Chem.* 1981; 256(7):3433-3442.
15. Kane WH, Davie EW. Blood coagulation factors V and VIII: structural and functional similarities and their relationship to hemorrhagic and thrombotic disorders. *Blood.* 1988;71(3):539-555.
16. Saenko EL, Shima M, Rajalakshmi KJ, Scandella D. A role for the C2 domain of factor VIII in binding to von Willebrand factor. *J Biol Chem.* 1994; 269(15):11601-11605.
17. Saenko EL, Scandella D. The acidic region of the factor VIII light chain and the C2 domain together form the high affinity binding site for von Willebrand factor. *J Biol Chem.* 1997;272(29): 18007-18014.
18. Saenko EL, Scandella D. A mechanism for inhibition of factor VIII binding to phospholipid by von Willebrand factor. *J Biol Chem.* 1995;270(23): 13826-13833.
19. Andersson LO, Brown JE. Interaction of factor VIII-von Willebrand Factor with phospholipid vesicles. *Biochem J.* 1981;200(1):161-167.
20. Lajmanovich A, Hudry-Clergeon G, Freyssinet JM, Marguerie G. Human factor VIII procoagulant activity and phospholipid interaction. *Biochim Biophys Acta.* 1981;678(1):132-136.
21. Gilbert GE, Kaufman RJ, Arena AA, Miao H, Pipe SW. Four hydrophobic amino acids of the factor VIII C2 domain are constituents of both the membrane-binding and von Willebrand factor-binding motifs. *J Biol Chem.* 2002;277(8): 6374-6381.
22. Gilbert GE, Novakovic VA, Kaufman RJ, Miao H, Pipe SW. Conservative mutations in the C2 domains of factor VIII and factor V alter phospholipid binding and cofactor activity. *Blood.* 2012;120(9):1923-1932.
23. Pratt KP, Shen BW, Takeshima K, Davie EW, Fujikawa K, Stoddard BL. Structure of the C2 domain of human factor VIII at 1.5 A resolution. *Nature.* 1999;402(6760):439-442.
24. Shen BW, Spiegel PC, Chang CH, et al. The tertiary structure and domain organization of coagulation factor VIII. *Blood.* 2008;111(3): 1240-1247.
25. Spiegel PC Jr, Jacquemin M, Saint-Remy JM, Stoddard BL, Pratt KP. Structure of a factor VIII C2 domain-immunoglobulin G4kappa Fab complex: identification of an inhibitory antibody epitope on the surface of factor VIII. *Blood.* 2001; 98(1):13-19.
26. Nogami K, Shima M, Hosokawa K, et al. Factor VIII C2 domain contains the thrombin-binding site responsible for thrombin-catalyzed cleavage at Arg1689. *J Biol Chem.* 2000;275(33): 25774-25780.
27. Nogami K, Shima M, Hosokawa K, et al. Role of factor VIII C2 domain in factor VIII binding to factor Xa. *J Biol Chem.* 1999;274(43): 31000-31007.
28. Nogami K, Shima M, Nishiya K, et al. Anticoagulant effects of a synthetic peptide containing residues Thr-2253-Gln-2270 within factor VIII C2 domain that selectively inhibits factor Xa-catalysed factor VIII activation. *Br J Haematol.* 2002;116(4):868-874.
29. Hsu TC, Pratt KP, Thompson AR. The factor VIII C1 domain contributes to platelet binding. *Blood.* 2008;111(1):200-208.
30. Lü J, Pipe SW, Miao H, Jacquemin M, Gilbert GE. A membrane-interactive surface on the factor VIII C1 domain cooperates with the C2 domain for cofactor function. *Blood.* 2011;117(11): 3181-3189.
31. Wakabayashi H, Griffiths AE, Fay PJ. Factor VIII lacking the C2 domain retains cofactor activity in vitro. *J Biol Chem.* 2010;285(33):25176-25184.
32. Prescott R, Nakai H, Saenko EL, et al; Recombinate and Kogenate Study Groups. The inhibitor antibody response is more complex in hemophilia A patients than in most nonhemophiliacs with factor VIII autoantibodies. *Blood.* 1997;89(10):3663-3671.
33. Arai M, Scandella D, Hoyer LW. Molecular basis of factor VIII inhibition by human antibodies. Antibodies that bind to the factor VIII light chain prevent the interaction of factor VIII with phospholipid. *J Clin Invest.* 1989;83(6): 1978-1984.
34. Jacquemin MG, Desqueper BG, Benhida A, et al. Mechanism and kinetics of factor VIII inactivation: study with an IgG4 monoclonal antibody derived from a hemophilia A patient with inhibitor. *Blood.* 1998;92(2):496-506.
35. Scandella D, Gilbert GE, Shima M, et al. Some factor VIII inhibitor antibodies recognize a common epitope corresponding to C2 domain amino acids 2248 through 2312, which overlap a phospholipid-binding site. *Blood.* 1995;86(5): 1811-1819.
36. Shima M, Nakai H, Scandella D, et al. Common inhibitory effects of human anti-C2 domain inhibitor alloantibodies on factor VIII binding to von Willebrand factor. *Br J Haematol.* 1995;91(3): 714-721.
37. Shima M, Scandella D, Yoshioka A, et al. A factor VIII neutralizing monoclonal antibody and a human inhibitor alloantibody recognizing epitopes in the C2 domain inhibit factor VIII binding to von Willebrand factor and to phosphatidylserine. *Thromb Haemost.* 1993; 69(3):240-246.
38. Meeks SL, Healey JF, Parker ET, Barrow RT, Lollar P. Antihuman factor VIII C2 domain antibodies in hemophilia A mice recognize a functionally complex continuous spectrum of epitopes dominated by inhibitors of factor VIII activation. *Blood.* 2007;110(13):4234-4242.
39. Meeks SL, Healey JF, Parker ET, Barrow RT, Lollar P. Nonclassical anti-C2 domain antibodies are present in patients with factor VIII inhibitors. *Blood.* 2008;112(4):1151-1153.
40. Meeks SL, Healey JF, Parker ET, Barrow RT, Lollar P. Non-classical anti-factor VIII C2 domain antibodies are pathogenic in a murine in vivo bleeding model. *J Thromb Haemost.* 2009;7(4): 658-664.
41. Walter JD, Werther RA, Polozova MS, et al. Characterization and solution structure of the factor VIII C2 domain in a ternary complex with classical and non-classical inhibitor antibodies. *J Biol Chem.* 2013;288(14):9905-9914.
42. Spiegel PC, Kaiser SM, Simon JA, Stoddard BL. Disruption of protein-membrane binding and identification of small-molecule inhibitors of coagulation factor VIII. *Chem Biol.* 2004;11(10): 1413-1422.
43. Spiegel PC, Murphy P, Stoddard BL. Surface-exposed hemophilic mutations across the factor VIII C2 domain have variable effects on stability and binding activities. *J Biol Chem.* 2004;279(51): 53691-53698.
44. Winn MD, Ballard CC, Cowtan KD, et al. Overview of the CCP4 suite and current developments. *Acta Crystallogr D Biol Crystallogr.* 2011;67(Pt 4): 235-242.
45. Adams PD, Afonine PV, Bunkóczi G, et al. PHENIX: a comprehensive Python-based system for macromolecular structure solution. *Acta Crystallogr D Biol Crystallogr.* 2010;66(Pt 2): 213-221.
46. Emsley P, Lohkamp B, Scott WG, Cowtan K. Features and development of Coot. *Acta Crystallogr D Biol Crystallogr.* 2010;66(Pt 4): 486-501.
47. Chen VB, Arendall WB III, Headd JJ, et al. MolProbity: all-atom structure validation for macromolecular crystallography. *Acta Crystallogr D Biol Crystallogr.* 2010;66(Pt 1):12-21.
48. Baker NA, Sept D, Joseph S, Holst MJ, McCammon JA. Electrostatics of nanosystems: application to microtubules and the ribosome. *Proc Natl Acad Sci USA.* 2001;98(18): 10037-10041.
49. Pettersen EF, Goddard TD, Huang CC, Couch GS, Greenblatt DM, Meng EC, Ferrin TE. UCSF Chimera—a visualization system for exploratory

research and analysis. *J Comput Chem.* 2004; 25(13):1605-1612.

50. Liu Z, Lin L, Yuan C, et al. Trp2313-His2315 of factor VIII C2 domain is involved in membrane binding: structure of a complex between the C2 domain and an inhibitor of membrane binding. *J Biol Chem.* 2010;285(12): 8824-8829.

51. Krissinel E, Henrick K. Inference of macromolecular assemblies from crystalline state. *J Mol Biol.* 2007;372(3):774-797.

52. Dimitrov JD, Roumenina LT, Plantier JL, et al. A human FVIII inhibitor modulates FVIII surface electrostatics at a VWF-binding site distant from its epitope. *J Thromb Haemost.* 2010;8(7): 1524-1531.

53. Soeda T, Nogami K, Ogiwara K, Shima M. Interactions between residues 2228-2240 within factor VIIIa C2 domain and factor IXa Gla domain contribute to propagation of clot formation. *Thromb Haemost.* 2011;106(5):893-900.

54. Soeda T, Nogami K, Nishiya K, et al. The factor VIIIa C2 domain (residues 2228-2240) interacts with the factor IXa Gla domain in the factor Xase complex. *J Biol Chem.* 2009;284(6):3379-3388.

55. Ngo JC, Huang M, Roth DA, Furie BC, Furie B. Crystal structure of human factor VIII: implications for the formation of the factor IXa-factor VIIIa complex. *Structure.* 2008;16(4):597-606.

56. Dimitrov JD, Christophe OD, Kang J, Repessé Y, Delignat S, Kaveri SV, Lacroix-Desmazes S. Thermodynamic analysis of the interaction of factor VIII with von Willebrand factor. *Biochemistry.* 2012;51(20):4108-4116.

57. Reding MT, Okita DK, Diethelm-Okita BM, Anderson TA, Conti-Fine BM. Human CD4+ T-cell epitope repertoire on the C2 domain of coagulation factor VIII. *J Thromb Haemost.* 2003;1(8):1777-1784.

58. Kasper CKAL, Counts RB, et al. Letter: A more uniform measurement of factor VIII inhibitors. *Thromb Diath Haemorrh.* 1975;34(3):869-872.

59. Hoyer LWGM, de la Fuente B. Immunochemical characterization of factor VIII inhibitors. In: Lw H, ed. *Factor VIII Inhibitors.* New York: Alan R. Liss; 1984:73-85.

60. Gawryl MS, Hoyer LW. Inactivation of factor VIII coagulant activity by two different types of human antibodies. *Blood.* 1982;60(5):1103-1109.